

## Journal Pre-proof

Comparison of  $^{68}\text{Ga}$ -labeled RGD mono- and multimers based on a clickable siderophore-based scaffold

Piriya Kaeopookum, Milos Petrik, Dominik Summer, Maximilian Klinger, Chuangyan Zhai, Christine Rangger, Roland Haubner, Hubertus Haas, Marian Hajduch, Clemens Decristoforo



PII: S0969-8051(19)30181-7

DOI: <https://doi.org/10.1016/j.nucmedbio.2019.09.002>

Reference: NMB 8090

To appear in: *Nuclear Medicine and Biology*

Received date: 12 July 2019

Revised date: 23 September 2019

Accepted date: 30 September 2019

Please cite this article as: P. Kaeopookum, M. Petrik, D. Summer, et al., Comparison of  $^{68}\text{Ga}$ -labeled RGD mono- and multimers based on a clickable siderophore-based scaffold, *Nuclear Medicine and Biology*(2019), <https://doi.org/10.1016/j.nucmedbio.2019.09.002>

This is a PDF file of an article that has undergone enhancements after acceptance, such as the addition of a cover page and metadata, and formatting for readability, but it is not yet the definitive version of record. This version will undergo additional copyediting, typesetting and review before it is published in its final form, but we are providing this version to give early visibility of the article. Please note that, during the production process, errors may be discovered which could affect the content, and all legal disclaimers that apply to the journal pertain.

© 2019 Published by Elsevier.

## Comparison of $^{68}\text{Ga}$ -labeled RGD mono- and multimers based on a clickable siderophore-based scaffold

Piriya Kaeopookum <sup>a,d</sup>, Milos Petrik <sup>b</sup>, Dominik Summer <sup>a</sup>, Maximilian Klinger <sup>a</sup>, Chuangyan Zhai <sup>a,e</sup>, Christine Rangger <sup>a</sup>, Roland Haubner <sup>a</sup>, Hubertus Haas <sup>c</sup>, Marian Hajduch <sup>b</sup>, Clemens Decristoforo <sup>a,\*</sup>

<sup>a</sup> *Department of Nuclear Medicine, Medical University Innsbruck, Innsbruck, Austria*

<sup>b</sup> *Institute of Molecular and Translational Medicine, Faculty of Medicine and Dentistry, Palacky University, Olomouc, Czech Republic*

<sup>c</sup> *Division of Molecular Biology, Biocenter, Medical University Innsbruck, Innsbruck, Austria*

<sup>d</sup> *Research and Development Division, Thailand Institute of Nuclear Technology, Nakhonnayok, Thailand*

<sup>e</sup> *School of Forensic Medicine, Southern Medical University, Guangzhou, China*

\* Corresponding author at: Universitätsklinik für Nuklearmedizin, Medizinische Universität Innsbruck, Anichstr. 35, A-6020 Innsbruck, Austria. Tel.: +43 512 504 80951; fax: +43 512 504 6780951.

*E-mail address:* [clemens.decristoforo@i-med.ac.at](mailto:clemens.decristoforo@i-med.ac.at) (C. Decristoforo).

**ABSTRACT**

Cyclic pentapeptides containing the amino acid sequence arginine-glycine-aspartic (RGD) have been widely applied to target  $\alpha_v\beta_3$  integrin, which is upregulated in various tumors during tumor-induced angiogenesis. Multimeric cyclic RGD peptides have been reported to be advantageous over monomeric counterparts for angiogenesis imaging. Here, we prepared mono-, di-, and trimeric cyclic arginine-glycine-aspartic-D-phenylalanine-lysine (c(RGDfK)) derivatives by conjugation with the natural chelator fusarinine C (FSC) using click chemistry based on copper (I)-catalyzed azide-alkyne cycloaddition (CuAAC). The  $\alpha_v\beta_3$  binding properties of  $^{68}\text{Ga}$ -labeled mono-, di-, and trimeric c(RGDfK) peptides were evaluated *in vitro* as well as *in vivo* and compared with the references monomeric [ $^{68}\text{Ga}$ ]GaNODAGA-c(RGDfK) and trimeric [ $^{68}\text{Ga}$ ]GaFSC(suc-c(RGDfK))<sub>3</sub>.

All  $^{68}\text{Ga}$ -labeled c(RGDfK) peptides displayed hydrophilicity ( $\log D = -2.96$  to  $-3.80$ ), low protein binding and were stable in phosphate buffered-saline (PBS) and serum up to 2 h. *In vitro* internalization assays with human melanoma M21 ( $\alpha_v\beta_3$ -positive) and M21-L ( $\alpha_v\beta_3$ -negative) cell lines showed specific uptake of all derivatives and increased in the series: mono- < di- < trimeric peptide. The highest tumor uptake, tumor-to-background ratios, and image contrast were found for the dimeric [ $^{68}\text{Ga}$ ]GaMAFC(c(RGDfK)aza)<sub>2</sub>.

In conclusion, we developed a novel strategy for direct, straight forward preparation of mono-, di-, and trimeric c(RGDfK) conjugates based on the FSC scaffold. Interestingly, the best  $\alpha_v\beta_3$  imaging properties were found for the dimeric [ $^{68}\text{Ga}$ ]GaMAFC(c(RGDfK)aza)<sub>2</sub>.

*Keywords: gallium-68, RGD, angiogenesis,  $\alpha_v\beta_3$  integrin, PET*

## 1. Introduction

Tumor angiogenesis is induced and exploited by tumor for providing oxygen and nutrients through newborn blood vessels. This process is well recognized as an essential mechanism for tumor growth and metastasis [1]. During angiogenesis,  $\alpha_v\beta_3$  integrins are overexpressed on angiogenic endothelial cells in pathological tissues but absent in normal endothelial cells and most healthy organs [2-4]. Moreover,  $\alpha_v\beta_3$  integrin shows recognition and high binding affinity with the arginine-glycine-aspartic (RGD) motif; hence,  $\alpha_v\beta_3$  is a target for tumor angiogenesis imaging.

Fluorine-18 labeled galacto-RGD ( $[^{18}\text{F}]$ galacto-RGD) was the first tracer for noninvasive imaging of  $\alpha_v\beta_3$  expression and was already evaluated in clinical trials [5]. This compound revealed good pharmacokinetics and receptor specific uptake. Due to the low yields and complex synthesis of  $[^{18}\text{F}]$ galacto-RGD, gallium-68 ( $^{68}\text{Ga}$ ) analogues were developed, initially based on 1,4,7,10-tetraazacyclododecane- $N,N',N'',N'''$ -tetraacetic acid (DOTA), followed by other bifunctional chelators (BFCs) like 1,4,7-triazacyclononane- $N,N',N''$ -triacetic acid (NOTA) and its derivative NODAGA exhibiting improved targeting properties for tumor angiogenesis [6-8].

To enhance the binding affinity toward  $\alpha_v\beta_3$ , multimerization of cyclic RGD peptides with various BFCs, linkers as well as different numbers of cyclic RGD motifs have been widely explored. New BFCs possessing three conjugation sites, 1,4,7-triazacyclononane- $N,N',N''$ -tris[(2-carboxyethyl)methylenephosphinic acid] (TRAP) and fusarinine C (FSC), were used for synthesis of trimeric cyclic RGD conjugates [9-11]. The hexadecimeric cyclic RGD is the multimer with the largest number of RGD motifs and showed a 125-fold increase of *in vitro* binding affinity relative to the monomer [12]. In most cases the increasing number of RGD

moieties revealed an enhanced binding affinity and improved tumour uptake as expected but also higher kidney uptake was observed [13,14].

Multimeric cyclic RGD peptides have been developed by two major routes. For the first strategy, cyclic RGD multimers (di-, tetra-, octa-, hexadecamer) were initially synthesized and subsequently linked to the conjugation site of BFCs such as DOTA, NOTA, and NODAGA [12-14]. It requires multi-step synthesis and purification as well as large amounts of c(RGD). For the second approach, chelating systems possessing multiple conjugation sites, including TRAP, FSC, and modified NOTA, were used as scaffold where one RGD moiety per each conjugation site was coupled [9,11,15,16]. The advantage of this approach is the straightforward synthesis route using the chelator not only for the complex formation but also as scaffold for the multimeric radiopharmaceutical. However, due to the broad availability of BFCs like DOTA or NOTA, the first approach is more commonly used.

In previous works, we reported that FSC, a cyclic hydroxamate siderophore, is a promising BFC for  $^{68}\text{Ga}$  and can be used as scaffold for multimerization [10,17,18]. FSC-based trimeric cyclic RGD with different linkers were synthesized.  $^{68}\text{Ga}$ ][Ga]FSC(suc-c(RGDfK))<sub>3</sub>, conjugate with succinic linker, exhibited better angiogenesis targeting properties than the monomeric  $^{68}\text{Ga}$ ][Ga]NODAGA-c(RGDfK) and the trimeric tracer with another BFC  $^{68}\text{Ga}$ ][Ga]TRAP(c(RGDfK))<sub>3</sub> [15]. We also showed the possibility to selectively introduce mono-, di-, and trisubstituents to FSC by acylation of the free amines [19,20].

In this study, FSC-based mono-, di-, and trimeric c(RGDfK) conjugates were synthesized using copper (I)-catalyzed azide-alkyne cycloaddition (CuAAC), a mild and high regioselective click reaction, and labeled with  $^{68}\text{Ga}$  (Scheme 1). Binding properties toward  $\alpha_v\beta_3$  integrin were studied *in vitro* and *in vivo*. MicroPET/CT images in tumor model of all conjugates were compared with

the references monomeric [ $^{68}\text{Ga}$ ]GaNODAGA-c(RGDfK) and trimeric [ $^{68}\text{Ga}$ ]GaFSC(suc-c(RGDfK))<sub>3</sub>.

## 2. Materials and methods

### 2.1. General

All commercially available chemicals were of analytical grade and used without further purification. Human melanoma M21 and M21-L cells were a kind gift from D.A. Cheresh, Departments of Immunology and Vascular Biology, The Scripps Research Institute, La Jolla, CA, USA. Human glioblastoma U87MG cells were obtained from American Type Culture Collection (ATCC, Manassas, VA, USA). The  $^{68}\text{Ge}/^{68}\text{Ga}$  generator (IGG100) was purchased from Eckert & Ziegler Strahlen- und Medizintechnik AG (Berlin, Germany) with a nominal activity of 1850 MBq and was eluted with 0.1 M HCl solution (Rotem Industries Ltd., Beer-Sheva, Israel) using the fractionated elution approach.

Reversed-phase high performance liquid chromatography (RP-HPLC) analysis was performed with an UltiMate 3000 UHPLC pump, an UltiMate 3000 autosampler, an UltiMate 3000 column compartment, an UltiMate 3000 variable wavelength detector (Thermo Fisher Scientific, Vienna, Austria) and a GabiStar radiometric detector (Raytest GmbH, Straubenhardt, Germany). An ACE 3 C<sub>18</sub>, 3  $\mu\text{m}$  100 Å, 150 x 3.0 mm column (ACE, Aberdeen, UK) and UV detection at 220 nm or 450 nm were employed. Acetonitrile (ACN)/H<sub>2</sub>O/0.1% trifluoroacetic acid (TFA) was used as mobile phase at a flow rate of 0.6 mL/min with the following multistep gradients: 0.0–1.0 min 10% ACN, 1.0–10.0 min 10–30% ACN, 10.0–11.0 min 30–60% ACN, 11.0–13.0 min 60% ACN (gradient A); and 0.0–1.0 min 10% ACN, 1.0–12.0 min 10–60% ACN, 12.0–14.0 min 60% ACN (gradient B).

Preparative RP-HPLC was carried out on a Gilson 322 HPLC pump with a Gilson UV/VIS-155 detector and a PrepFC automatic collector (Gilson International B.V., Limburg, Germany). A Eurosil Bioselect Vertex Plus, C<sub>18A</sub> 5µm 300 Å, 30 × 8 mm precolumn and a Eurosil Bioselect Vertex Plus, C<sub>18A</sub> 5µm 300 Å, 300 × 8 mm column (Knauer, Berlin, Germany) were employed with a flow rate of 2 mL/min and UV detection at 220 nm. The mobile phase ACN/H<sub>2</sub>O/0.1% TFA was used with several multistep gradients.

Radio-instant thin layer chromatography (radio-ITLC) was analyzed on a TLC scanner (ScanRAM, LabLogistic, Sheffield, UK) using TLC-SG strips (Varian, Lake Forest, CA, USA) with two different mobile phases: 0.1 M sodium citrate (pH 5) and 1:1 (v/v) mixture of 1 M ammonium acetate (NH<sub>4</sub>OAc) and methanol (MeOH) (pH 7).

The radioactivities of *in vitro* and *in vivo* samples were measured in a 2480 Automatic Gamma Counter Wizard<sup>2</sup> 3" (PerkinElmer, Waltham, MA, USA).

## 2.2. [Fe]Fusarinine C ([Fe]FSC)

[Fe]FSC was extracted from *Aspergillus fumigatus* mutant strain *ΔsidG*. Fungi were cultured under iron starvation condition as described by Schrettl et al. [21] with slightly changed incubation time and extraction method as previously published [16]. [Fe]FSC:  $t_R = 6.3$  min (gradient A). MALDI TOF-MS:  $m/z$  [M + H]<sup>+</sup> = 780.55 [C<sub>33</sub>H<sub>51</sub>FeN<sub>6</sub>O<sub>12</sub>; exact mass: 779.63 (calculated)].

## 2.3. [Fe]MAFC and [Fe]DAFC

To limit the reaction site from three to two or one positions, one or two amino groups of [Fe]FSC were acetylated to give acetyl[Fe]FSC ([Fe]MAFC) or diacetyl[Fe]FSC ([Fe]DAFC), respectively, as previously described [19]. [Fe]MAFC: 1.9 mg, 8% yield,  $t_R = 7.80$  min (gradient

A), MALDI TOF-MS:  $m/z$   $[M + Na]^+ = 844.65$   $[C_{35}H_{53}FeN_6O_{13}$ ; exact mass: 821.67 (calculated)]. [Fe]DAFC: 7.9 mg, 32% yield,  $t_R = 9.36$  min (gradient A), MALDI TOF-MS:  $m/z$   $[M + Na]^+ = 886.68$   $[C_{37}H_{55}FeN_6O_{14}$ ; exact mass: 863.71 (calculated)].

#### 2.4. [Fe]DAFC(alkyn), [Fe]MAFC(alkyn)<sub>2</sub>, and [Fe]FSC(alkyn)<sub>3</sub>

The coupling reagents 1-hydroxy-7-azabenzotriazole (HOAt) and *O*-(7-azabenzotriazol-1-yl)-*N,N,N',N'*-tetramethyl uroniumhexafluorophosphate (HATU) were mixed with 4-pentynoic acid in dimethylformamide (DMF) in a molar ratio of 4:4:3. The mixture with an excess of 1.5, 3, or 4.5 equiv of 4-pentynoic acid was transferred to 1 equiv of [Fe]DAFC (5.9 mg, 6.9  $\mu$ mol), [Fe]MAFC (14.5 mg, 17.7  $\mu$ mol), or [Fe]FSC (9.9 mg, 12.7  $\mu$ mol), respectively. *N,N*-diisopropylethylamine (DIPEA) was added to adjust pH to 10–11, and the reaction mixture was stirred at RT for 1 h. Hereafter solvent was reduced *in vacuo*, and crude product was then purified by preparative RP-HPLC followed by lyophilization to obtain pentynoyl[Fe]DAFC ([Fe]DAFC(alkyn)), dipentynoyl[Fe]MAFC ([Fe]MAFC(alkyn)<sub>2</sub>), or tripentynoyl[Fe]FSC ([Fe]FSC(alkyn)<sub>3</sub>). [Fe]DAFC(alkyn): 4.2 mg, 64% yield,  $t_R = 8.63$  min (gradient B), MALDI TOF-MS:  $m/z$   $[M + H]^+ = 944.44$   $[C_{42}H_{59}FeN_6O_{15}$ ; exact mass: 943.79 (calculated)]. [Fe]MAFC(alkyn)<sub>2</sub>: 10.13 mg, 58% yield,  $t_R = 9.57$  min (gradient B), MALDI TOF-MS:  $m/z$   $[M + H]^+ = 982.53$   $[C_{45}H_{61}FeN_6O_{15}$ ; exact mass: 981.84 (calculated)]. [Fe]FSC(alkyn)<sub>3</sub>: 7.3 mg, 57% yield,  $t_R = 10.78$  min (gradient B), MALDI TOF-MS:  $m/z$   $[M + Na]^+ = 1042.65$   $[C_{48}H_{63}FeN_6O_{15}$ ; exact mass: 1019.89 (calculated)].

#### 2.5. Cyclo(-Arg(Pbf)-Gly-Asp(OtBu)-D-Phe-Lys-)

Synthesis of cyclo(-Arg(Pbf)-Gly-Asp(OtBu)-D-Phe-Lys-) was performed as described by Haubner et al [22,23]. Briefly, cyclic pentapeptides with side chain protecting groups, cyclo(-Arg(Pbf)-Gly-Asp(OtBu)-D-Phe-Lys(Dde)-), was synthesized by cyclization of linear

pentapeptides from Fmoc-based solid-phase peptide synthesis (SPPS). To obtain free amino group at lysine for further conjugation, selective deprotection of Dde was carried out using 2% hydrazine in DMF. Purifications were performed by trituration with H<sub>2</sub>O followed by preparative RP-HPLC. Cyclo(-Arg(Pbf)-Gly-Asp(OtBu)-D-Phe-Lys-): 146.7 mg, 74% yield (based on linear pentapeptide),  $t_R = 12.38$  min (gradient B). MALDI TOF-MS:  $m/z$  [M + H]<sup>+</sup> = 912.64 [C<sub>44</sub>H<sub>65</sub>N<sub>9</sub>O<sub>10</sub>S; exact mass: 912.10 (calculated)].

#### 2.6. Cyclo(-Arg(Pbf)-Gly-Asp(OtBu)-D-Phe-Lys(N<sub>3</sub>-)

To cyclo(-Arg(Pbf)-Gly-Asp(OtBu)-D-Phe-Lys-) (30.6 mg, 33.6 μmol), the mixture of HOAt (9.1 mg, 67.1 μmol), HATU (25.6 mg, 67.1 μmol), and 5-azidopentanoic acid (7.2 mg, 50.4 μmol) in DMF was added. The reaction mixture was alkalized to pH 10–11 using DIPEA and stirred at RT for 30 min. Solvent was evaporated, and residual was separated by preparative RP-HPLC. Cyclo(-Arg(Pbf)-Gly-Asp(OtBu)-D-Phe-Lys(N<sub>3</sub>-): 22.7 mg, 65% yield,  $t_R = 14.86$  min (gradient B). MALDI TOF-MS:  $m/z$  [M + H]<sup>+</sup> = 1038.51 [C<sub>49</sub>H<sub>72</sub>N<sub>12</sub>O<sub>11</sub>S; exact mass: 1037.23 (calculated)].

#### 2.7. Cyclo(-Arg-Gly-Asp-D-Phe-Lys(N<sub>3</sub>-)

Cyclo(-Arg(Pbf)-Gly-Asp(OtBu)-D-Phe-Lys(N<sub>3</sub>-) (22.7 mg, 21.9 μmol) was dissolved in the solution of TFA/H<sub>2</sub>O/isopropylsilane (38:1:1 v/v) and stirred at RT. After 4 h, the reaction mixture was dried *in vacuo*, and crude product was obtained by trituration with diethyl ether. Hereon purification was performed on preparative RP-HPLC. Cyclo(-Arg-Gly-Asp-D-Phe-Lys(N<sub>3</sub>-) (c(RGDfK)N<sub>3</sub>): 11.0 mg, 69% yield,  $t_R = 8.79$  min (gradient B). MALDI TOF-MS:  $m/z$  [M + H]<sup>+</sup> = 729.08 [C<sub>32</sub>H<sub>48</sub>N<sub>12</sub>O<sub>8</sub>; exact mass: 728.80 (calculated)].

#### 2.8. DAFC(c(RGDfK)aza), MAFC(c(RGDfK)aza)<sub>2</sub>, and FSC(c(RGDfK)aza)<sub>3</sub>

DMF solution of 1 equiv [Fe]DAFC(alkyn) (1.83 mg, 1.94  $\mu\text{mol}$ ), [Fe]MAFC(alkyn)<sub>2</sub> (1.78 mg, 1.81  $\mu\text{mol}$ ), or [Fe]FSC(alkyn)<sub>3</sub> (1.66 mg, 1.63  $\mu\text{mol}$ ) were mixed with 2, 4, or 6 equiv of c(RGDfK)N<sub>3</sub>, respectively. A freshly prepared mixture of tris(3-hydroxypropyltriazolylmethyl)amine (THPTA) (10 equiv) and CuSO<sub>4</sub>·5H<sub>2</sub>O (4 equiv) in H<sub>2</sub>O was added to the DMF mixture followed by sodium ascorbate (200 equiv) solution. After stirring at RT for 2 h, 100 equiv of disodium ethylenediaminetetraacetic acid (Na<sub>2</sub>EDTA) solution (50 mM, pH 4) was added to remove iron from molecules, and the reaction mixture was stirred for a further 18 h. After solvent removal, the crude product was purified by preparative RP-HPLC. DAFC(c(RGDfK)aza): 1.2 mg, 37% yield,  $t_R$  = 12.68 min (gradient A). MALDI TOF-MS:  $m/z$  [M + H]<sup>+</sup> = 1620.24 [C<sub>74</sub>H<sub>110</sub>N<sub>18</sub>O<sub>23</sub>; exact mass: 1619.77 (calculated)]. MAFC(c(RGDfK)aza)<sub>2</sub>: 1.3 mg, 30% yield,  $t_R$  = 12.82 min (gradient A). MALDI TOF-MS:  $m/z$  [M + H]<sup>+</sup> = 2386.83 [C<sub>109</sub>H<sub>160</sub>N<sub>30</sub>O<sub>31</sub>; exact mass: 2386.61 (calculated)]. FSC(c(RGDfK)aza)<sub>3</sub>: 1.59 mg, 31% yield,  $t_R$  = 9.15 min (gradient B). MALDI TOF-MS:  $m/z$  [M + Na]<sup>+</sup> = 3177.13 [C<sub>144</sub>H<sub>210</sub>N<sub>42</sub>O<sub>39</sub>; exact mass: 3153.46 (calculated)].

### 2.9. NODAGA-c(RGDfK) and FSC(suc-c(RGDfK))<sub>3</sub>

Compounds were synthesized as described by Knetsch et al [7,10].

### 2.10. <sup>68</sup>Ga-Labeling

To 5  $\mu\text{g}$  of peptide, 200  $\mu\text{L}$  [<sup>68</sup>Ga]GaCl<sub>3</sub> (approx. 35–40 MBq) in 0.1 M HCl (fractionated elution) was added. The pH of solution was adjusted to 4.5 by adding 40  $\mu\text{L}$  of 1.1 M sodium acetate (NaOAc). The labeling mixture was allowed at RT for 10 min. Radiochemical yield (% RCY) of [<sup>68</sup>Ga]GaDAFC(c(RGDfK)aza), [<sup>68</sup>Ga]GaMAFC(c(RGDfK)aza)<sub>2</sub>, and [<sup>68</sup>Ga]GaFSC(c(RGDfK)aza)<sub>3</sub> were determined using RP-HPLC and/or radio-ITLC.

### 2.11. <sup>nat</sup>Ga-Complexation

Gallium-complexes of all conjugates were synthesized using the same protocol as described for  $^{68}\text{Ga}$ -labeling whereby  $[\text{}^{68}\text{Ga}]\text{GaCl}_3$  was replaced by 100-fold molar excess of  $\text{GaBr}_3$  in 200  $\mu\text{L}$  of 0.1 N HCl.

### 2.12. Distribution coefficient ( $\log D$ )

$[\text{}^{68}\text{Ga}]\text{GaDAFC}(\text{c}(\text{RGDfK})\text{aza})$ ,  $[\text{}^{68}\text{Ga}]\text{GaMAFC}(\text{c}(\text{RGDfK})\text{aza})_2$ , or  $[\text{}^{68}\text{Ga}]\text{GaFSC}(\text{c}(\text{RGDfK})\text{aza})_3$  (1  $\mu\text{M}$ ) in 500  $\mu\text{L}$  phosphate buffered-saline (PBS) were mixed with 500  $\mu\text{L}$  octanol. The mixture was vortexed at 1400 rpm for 15 min and subsequently centrifuged at 2000 rcf for 2 min. Aliquots of aqueous and octanol phases were separately collected and measured in a gamma counter. The  $\log D$  values were calculated from the obtained data ( $n = 6$ ).

### 2.13. Stability assay

Stabilities of all three conjugates were tested in PBS (pH 7.4) and fresh human serum after 0, 30, 60, and 120 min incubation.  $[\text{}^{68}\text{Ga}]\text{GaDAFC}(\text{c}(\text{RGDfK})\text{aza})$ ,  $[\text{}^{68}\text{Ga}]\text{GaMAFC}(\text{c}(\text{RGDfK})\text{aza})_2$ , or  $[\text{}^{68}\text{Ga}]\text{GaFSC}(\text{c}(\text{RGDfK})\text{aza})_3$  (50  $\mu\text{L}$ , 2 nmol) were incubated in 450  $\mu\text{L}$  PBS or human serum at 37 °C. Hereon, aliquots of PBS were injected directly to RP-HPLC while serum aliquots were mixed with MeOH, vortexed, and centrifuged at 20000 rcf for 2 min. Supernatant was diluted with  $\text{H}_2\text{O}$  and subsequently analyzed by RP-HPLC. The stability was presented as radiochemical purity (% RCP) of radiotracer ( $n = 3$ ).

### 2.14. Protein binding assay

Protein binding abilities were carried out by incubating  $[\text{}^{68}\text{Ga}]\text{GaDAFC}(\text{c}(\text{RGDfK})\text{aza})$ ,  $[\text{}^{68}\text{Ga}]\text{GaMAFC}(\text{c}(\text{RGDfK})\text{aza})_2$ , and  $[\text{}^{68}\text{Ga}]\text{GaFSC}(\text{c}(\text{RGDfK})\text{aza})_3$  in human serum at 37 °C for 30, 60, and 120 min. After incubation, 25  $\mu\text{L}$  of serum aliquot was passed through a size exclusion spin columns MicroSpin<sup>TM</sup> G-50 (GE Healthcare, Vienna, Austria) by centrifugation at

2000 ref for 2 min. Protein binding ability was determined by measuring activities of eluate (protein bound) and column (non-protein bound) in a gamma counter. The results were displayed as percentage of protein bound to total activity ( $n = 3$ ).

### 2.15. Receptor binding affinity assay

The half maximal inhibitory concentration ( $IC_{50}$ ) of [ $^{nat}Ga$ ]DAFC(c(RGDfK)aza), [ $^{nat}Ga$ ]MAFC(c(RGDfK)aza)<sub>2</sub>, [ $^{nat}Ga$ ]FSC(c(RGDfK)aza)<sub>3</sub> and a control cyclo(-Arg-Gly-Asp-D-Tyr-Val-) (c(RGDyV)) for binding  $\alpha_v\beta_3$  integrin were evaluated in human melanoma M21 ( $\alpha_v\beta_3$ -positive) cells using [ $^{125}I$ ]c(RGDyV) as radioligand. [ $^{125}I$ ]c(RGDyV) was produced as described previously [22]. M21 cells were washed twice with PBS (pH 7.4) and then suspended in binding buffer (20 mM tris(hydroxymethyl)aminomethane (TRIS), 0.1% bovine serum albumin (BSA), 1 mM CaCl<sub>2</sub>, 1 mM MgCl<sub>2</sub>, 10  $\mu$ M MnCl<sub>2</sub>, 150 mM NaCl, pH 7.3) at a concentration of  $1 \times 10^7$  cells/mL. In a 96-well MultiScreen Filter Plates HTS (1  $\mu$ m glass fiber filter, Merck Millipore, Darmstadt, Germany), aliquots of  $10^6$  cells were added and incubated in increasing concentration [0.001–1000 nM] of [ $^{nat}Ga$ ]-bound conjugates or c(RGDyV) in triplicate. After 5 min, [ $^{125}I$ ]c(RGDyV) (approx. 50000 cpm) was added and cells were incubated at 37 °C for 2 h under shaking condition (200 rpm). The incubation was interrupted by suction of the medium and the plate was washed thrice with ice-cold binding buffer. The filters were collected and the remaining activities were measured in a gamma counter.  $IC_{50}$  values were calculated using a nonlinear curve fitting in OriginPro 6.1 software (Northampton, MA, USA).

### 2.16. Internalization assay

Cell suspensions were prepared at a concentration of  $2 \times 10^6$  cells/mL for human melanoma M21 ( $\alpha_v\beta_3$ -positive) as well as M21-L ( $\alpha_v\beta_3$ -negative) and  $6 \times 10^6$  cells/0.2 mL for U87MG cells, in RPMI 1640 (Gibco, Invitrogen Corporation, Paisley, UK) containing 1% glutamine, 1%

BSA, 1 mM CaCl<sub>2</sub>, 1 mM MgCl<sub>2</sub>, and 10 μM MnCl<sub>2</sub>. Aliquots of 1 mL of M21 and M21-L cells or 0.2 mL of U87MG were transferred to Eppendorf tubes in triplicate for each cell line with either PBS/0.5% BSA (total series) or c(RGDyV) in PBS/0.5% BSA with a final concentration of 10 μM (nonspecific series) and incubated at 37 °C for 1 h. After adding 50 μL [<sup>68</sup>Ga]GaDAFC(c(RGDfK)aza), [<sup>68</sup>Ga]GaMAFC(c(RGDfK)aza)<sub>2</sub>, or [<sup>68</sup>Ga]GaFSC(c(RGDfK)aza)<sub>3</sub> to a final concentration of 10 nM, cells were incubated at 37 °C for 90 min. Incubation was interrupted by centrifugation at 5000 rpm for 2 min, medium removal, and rapid rinsing twice with ice-cold TRIS buffer (25 mM TRIS, 0.1% BSA, 1 mM CaCl<sub>2</sub>, 1 mM MgCl<sub>2</sub>, 10 μM MnCl<sub>2</sub>, 150 mM NaCl, pH 7.3). Thereafter, cells were incubated twice with acid wash buffer (20 mM sodium acetate buffer, pH 4.5) at 37 °C for 5 min to wash out surface-bound molecules, and supernatant was collected. Subsequently, cells were lysed by treatment twice with 2 M NaOH, and fractions were combined (internalized fraction). All collected samples and standard solutions were counted by a gamma counter. Protein amount in NaOH fraction was determined using spectrophotometric analysis with Bradford reagent (Sigma-Aldrich). Internalized activity was expressed as percentage of total activity per milligram protein (% cpm/mg protein).

### 2.17. Animal experiment

All animal experiments were conducted in accordance with regulations and guidelines of the Czech Animal Protection Act (No. 246/1992), and with the approval of the Czech Ministry of Education, Youth, and Sports (MSMT-16402/2012-30), and the institutional Animal Welfare Committee of the Faculty of Medicine and Dentistry of Palacky University in Olomouc.

Female 8–10-week-old SCID mice (Envigo, Horst, The Netherlands) were used for *in vivo* experiments. The number of animals was reduced as much as possible ( $n = 3$  per group and time

point) in all experiments. Tumor xenografts were established near the front shoulder of SCID mice by subcutaneous injection of human glioblastoma U87MG ( $\alpha_v\beta_3$ -positive),  $5 \times 10^6$  cells in 200  $\mu$ L appropriate medium and Matrigel (1:1). The tumors were allowed to grow until 0.5 cm<sup>3</sup>. The tracer injection and small animal imaging were carried out under 2% isoflurane anaesthesia (FORANE, Abbott Laboratories, Abbott Park, IL, USA) to minimize animal suffering and to prevent animal motion.

### 2.17.1. Biodistribution studies

To evaluate *ex vivo* biodistribution, a group of 3 tumor-bearing mice were retro-orbitally (r.o.) injected with [<sup>68</sup>Ga]GaDAFC(c(RGDfK)aza), [<sup>68</sup>Ga]GaMAFC(c(RGDfK)aza)<sub>2</sub>, [<sup>68</sup>Ga]GaFSC(c(RGDfK)aza)<sub>3</sub>, [<sup>68</sup>Ga]GaFSC(suc-c(RGDfK))<sub>3</sub>, or [<sup>68</sup>Ga]GaNODAGA-c(RGDfK) (1–2 MBq/mouse, 1  $\mu$ g peptide). Animals were sacrificed by cervical dislocation at 30 or 90 min post-injection (p.i.) for all tracers except [<sup>68</sup>Ga]GaFSC(suc-c(RGDfK))<sub>3</sub> which was studied only for 90 min p.i. Organs and tissues (blood, spleen, pancreas, stomach, intestines, kidneys, liver, heart, lung, muscle, femur, tumor) were collected, weighed, and measured in a gamma counter. Results were expressed as percentage of injected dose per gram tissue (%ID/g).

### 2.17.2. MicroPET/CT imaging

MicroPET and CT images were acquired with an Albira PET/SPECT/CT small animal imaging system (Bruker Biospin Corporation, Woodbridge, CT, USA). Xenograft-bearing mice were injected r.o. with [<sup>68</sup>Ga]GaDAFC(c(RGDfK)aza), [<sup>68</sup>Ga]GaMAFC(c(RGDfK)aza)<sub>2</sub>, or [<sup>68</sup>Ga]GaFSC(c(RGDfK)aza)<sub>3</sub> in a dose of 5–8 MBq corresponding to 1–2  $\mu$ g of peptide per animal. Anaesthetized animals were placed in prone position in the Albira system before the start of imaging. Static PET/CT images were acquired over 40 min starting 90 min after injection. A 10-min PET scan (axial FOV 148 mm) was performed, followed by a double CT scan (axial

FOV 110 mm, 45 kVp, 400  $\mu$ A, at 400 projections). Scans were reconstructed with the Albira software (Bruker Biospin Corporation, Woodbridge, CT, USA) using the maximum likelihood expectation maximization (MLEM) and filtered backprojection (FBP) algorithms. After reconstruction, acquired data was viewed and analyzed with PMOD software (PMOD Technologies Ltd., Zurich, Switzerland).

### 2.18. Statistical analysis

Differences in tumor uptake among the 5 c(RGDfK) peptides were analyzed using GraphPad Prism 8.1.1 (GraphPad Software Inc.; La Jolla, USA) with a one-way ANOVA followed by a Holm-Sidak post hoc test for multiple comparison. The level of significant was set to a *P* value of less than 0.05.

## 3. Results

### 3.1. Peptide synthesis and coupling to the chelators

Synthesis of deprotected cyclo(-Arg-Gly-Asp-D-Phe-Lys(N<sub>3</sub>)-) (c(RGDfK)N<sub>3</sub>) using Fmoc protocols, cyclization, deprotection of lysine side chain, azido introduction, and deprotection of all protecting groups was carried out in good yield. Mono-, di-, and trimeric c(RGDfK) were achieved from CuAAC of c(RGDfK)N<sub>3</sub> and alkyne siderophores in moderate yields. Straightforward synthesis of all conjugates is presented in Scheme 1.

### 3.2. <sup>68</sup>Ga-Labeling

At the stated labeling conditions (pH 4.5; RT; 10 min incubation), [<sup>68</sup>Ga]GaDAFC(c(RGDfK)aza), [<sup>68</sup>Ga]GaMAFC(c(RGDfK)aza)<sub>2</sub>, and [<sup>68</sup>Ga]GaFSC(c(RGDfK)aza)<sub>3</sub> were obtained in almost quantitative % RCP (> 99%) and used without further purification.

### 3.3. *In vitro* characterization

Log $D$  values of all three conjugates revealed high hydrophilicity. Conjugates with less c(RGDfK) motifs showed higher hydrophilicity as follows: [ $^{68}\text{Ga}$ ]GaDAFC(c(RGDfK)aza) ( $-3.80 \pm 0.06$ ) > [ $^{68}\text{Ga}$ ]GaMAFC(c(RGDfK)aza) $_2$  ( $-3.54 \pm 0.11$ ) > [ $^{68}\text{Ga}$ ]GaFSC(c(RGDfK)aza) $_3$  ( $-2.96 \pm 0.21$ ).

Stability studies in PBS (pH 7.4) and human serum at 37 °C revealed high stability for all compounds in both media for up to 2 h (see Table 1).

Incubation of all [ $^{68}\text{Ga}$ ]-labeled c(RGDfK)aza in human serum exhibited low protein binding between 3–9% of total activity. Compounds with less number of c(RGDfK) peptide showed lower values ([ $^{68}\text{Ga}$ ]GaDAFC(c(RGDfK)aza) < [ $^{68}\text{Ga}$ ]GaMAFC(c(RGDfK)aza) $_2$  < [ $^{68}\text{Ga}$ ]GaFSC(c(RGDfK)aza) $_3$ ) at any time point.

Binding affinities to  $\alpha_v\beta_3$  integrin of metal bound mono-, di-, and trimeric c(RGDfK) conjugates are shown in Fig. 1. IC $_{50}$  values from displacement assays using M21 cells with increasing concentration of the inhibitory peptides were  $17.0 \pm 0.8$  nM for c(RGDyV) (control),  $80.3 \pm 2.0$  nM for [ $^{nat}\text{Ga}$ ]DAFC(c(RGDfK)aza),  $3.9 \pm 1.2$  nM for [ $^{nat}\text{Ga}$ ]MAFC(c(RGDfK)aza) $_2$ , and  $1.7 \pm 0.2$  nM for [ $^{nat}\text{Ga}$ ]FSC(c(RGDfK)aza) $_3$ . These results revealed the enhancement of binding affinity with increasing number of RGD binding motifs.

Results from *In vitro* internalization studies using M21 ( $\alpha_v\beta_3$ -positive) and M21-L ( $\alpha_v\beta_3$ -negative) cells are presented in Fig. 2. The internalized activities (% cpm/mg protein) in M21 cells without blockade were extended with increasing number of c(RGDfK) moiety,  $2.2 \pm 0.3$  for [ $^{68}\text{Ga}$ ]GaDAFC(c(RGDfK)aza),  $4.5 \pm 0.8$  for [ $^{68}\text{Ga}$ ]GaMAFC(c(RGDfK)aza) $_2$ , and  $9.8 \pm 1.0$  for [ $^{68}\text{Ga}$ ]GaFSC(c(RGDfK)aza) $_3$ . The corresponding activities in M21 cells with blockade and M21-L cells with or without blockade were reduced to 0.2 to 0.7% confirming the receptor-

specific internalization of all compounds. In U87MG cells, corresponding values were considerably lower with  $1.2 \pm 0.1$ ,  $2.9 \pm 0.3$ , and  $2.6 \pm 0.1$ , for [ $^{68}\text{Ga}$ ]GaDAFC(c(RGDfK)aza), [ $^{68}\text{Ga}$ ]GaMAFC(c(RGDfK)aza)<sub>2</sub>, and [ $^{68}\text{Ga}$ ]GaFSC(c(RGDfK)aza)<sub>3</sub>, respectively, blocking reduced the values to 0.9–1.4%. (see Supporting Information Fig. S1).

### 3.4. Biodistribution studies

Biodistribution data and tumor-to-tissue ratios of all three studied and two reference  $^{68}\text{Ga}$ -labeled c(RGDfK) compounds in tumor-bearing SCID mice at 90 min p.i. are presented in Fig. 3 and Fig. 4, respectively. The results found in this study differed from *in vitro* evaluations. The tumor uptake was as follows: [ $^{68}\text{Ga}$ ]GaMAFC(c(RGDfK)aza)<sub>2</sub> > [ $^{68}\text{Ga}$ ]GaFSC(c(RGDfK)aza)<sub>3</sub> > [ $^{68}\text{Ga}$ ]GaDAFC(c(RGDfK)aza). Among the studied compounds, monomeric [ $^{68}\text{Ga}$ ]GaDAFC(c(RGDfK)aza) showed the lowest tumor uptake ( $2.73 \pm 0.28$  %ID/g) as expected. This value was 2-fold, but not significantly ( $P = 0.2$ ), higher than that of the reference [ $^{68}\text{Ga}$ ]GaNODAGA-c(RGDfK) ( $1.35 \pm 0.39$  %ID/g) while uptakes in all the rest organs were comparable. Trimeric [ $^{68}\text{Ga}$ ]GaFSC(c(RGDfK)aza)<sub>3</sub> revealed similar activity accumulations in tumor ( $3.98 \pm 0.64$  %ID/g) and all other tissues, except spleen, relative to standard trimeric [ $^{68}\text{Ga}$ ]GaFSC(suc-c(RGDfK))<sub>3</sub> ( $4.95 \pm 1.10$  %ID/g). Surprisingly, dimeric [ $^{68}\text{Ga}$ ]GaMAFC(c(RGDfK)aza)<sub>2</sub> exhibited unexpected high tumor uptake ( $8.19 \pm 0.41$  %ID/g), which was significantly higher than that of the trimeric [ $^{68}\text{Ga}$ ]GaFSC(c(RGDfK)aza)<sub>3</sub> ( $P = 0.003$ ) and [ $^{68}\text{Ga}$ ]GaFSC(suc-c(RGDfK))<sub>3</sub> ( $P = 0.02$ ). All radiolabeled compounds showed fast blood clearance (< 0.3 %ID/g) but high accumulation in kidneys. Highest uptake in each organ was mostly found for [ $^{68}\text{Ga}$ ]GaFSC(c(RGDfK)aza)<sub>3</sub>. Statistical comparison of tumor uptakes among the 5 conjugates is presented in Supporting Information, Fig. S2.

Tumor-to-background ratios (Fig. 4), neglecting tumor-to-spleen ratios which were comparable in all compounds and tumor-to-femur which was lowest in [ $^{68}\text{Ga}$ ]GaNODAGAc(RGDfK), were ranked as follows: [ $^{68}\text{Ga}$ ]GaMAFC(c(RGDfK)aza) $_2$  > [ $^{68}\text{Ga}$ ]GaDAFC(c(RGDfK)aza) > [ $^{68}\text{Ga}$ ]GaFSC(suc-c(RGDfK)) $_3$  ~ [ $^{68}\text{Ga}$ ]GaNODAGAc(RGDfK) ~ [ $^{68}\text{Ga}$ ]GaFSC(c(RGDfK)aza) $_3$ . The same trend was also observed at 30 min p.i. (See. Supporting Information, Fig. S3). Moreover, [ $^{68}\text{Ga}$ ]GaMAFC(c(RGDfK)aza) $_2$  revealed excellent tumor-to-blood ratio ( $44.38 \pm 5.58$ ) which was 2.7-fold higher than [ $^{68}\text{Ga}$ ]GaFSC(c(RGDfK)aza) $_3$  ( $16.56 \pm 1.35$ ). [ $^{68}\text{Ga}$ ]GaFSC(c(RGDfK)aza) $_3$  showed the lowest ratios in all organs due to its high retention especially in kidneys.

### 3.5. MicroPET/CT imaging

MicroPET/CT imaging was performed in SCID mice bearing U87MG tumor to compare the image properties and *in vivo* pharmacokinetic of mono-, di-, and trimeric counterparts (Fig. 5). The visualization intensities of all studied conjugates in tumor followed the order of: [ $^{68}\text{Ga}$ ]GaMAFC(c(RGDfK)aza) $_2$  > [ $^{68}\text{Ga}$ ]GaDAFC(c(RGDfK)aza) > [ $^{68}\text{Ga}$ ]GaFSC(c(RGDfK)aza) $_3$  while intensities in kidneys were as follows: [ $^{68}\text{Ga}$ ]GaFSC(c(RGDfK)aza) $_3$  > [ $^{68}\text{Ga}$ ]GaMAFC(c(RGDfK)aza) $_2$  > [ $^{68}\text{Ga}$ ]GaDAFC(c(RGDfK)aza). These results confirmed the tumor-targeting abilities and kidney retentions found in *ex vivo* biodistribution studies (Fig. 3). Besides the tumor and kidneys, urinary bladder showed intense visualization, confirming the main elimination route *via* renal excretion.

## 4. Discussion

The first  $^{68}\text{Ga}$ -labeled cyclic RGD compounds for PET/CT imaging of  $\alpha_v\beta_3$  integrin expression were [ $^{68}\text{Ga}$ ]GaDOTA-c(RGDfK) and [ $^{68}\text{Ga}$ ]GaNOTA-c(RGDyK) [6,24] showing the potential to image angiogenesis. To improve image contrast by enhancing the binding affinity to  $\alpha_v\beta_3$  integrin, multivalent concepts have been applied by several research groups and showed an enhanced localization of multimeric cyclic RGD peptides in  $\alpha_v\beta_3$  integrin-expressing tumors [13,14,25]. Most multivalent peptides were di- and tetrameric cyclic RGD peptides employing DOTA and NOTA as BFCs. Comparison to the monomeric RGD counterpart, both di- and tetrameric conjugates displayed improved tumor targeting due to their avidity effect, enhanced statistical rebinding, and prolonged target retention from increased tracer concentration. Nonetheless, dimeric c(RGD) was superior to tetrameric c(RGD) analogues in term of tumor-to-tissue ratios due to the slower elimination from non-target tissues of the larger tetrameric molecules [14,26]. Recently, several groups have described the use of azide or alkyne derivatized scaffolds based on the TRAP [27], DOTA [28], and HBED-CC [29], for multiple conjugation of targeting moieties through CuAAC click chemistry, a method for highly selective reaction under mild condition.

In this work, we successfully developed novel mono-, di-, and trimeric c(RGDfK) probes based on the FSC scaffold applying CuAAC click chemistry as an alternative conjugation strategy. We compared them with previously published conjugates, [ $^{68}\text{Ga}$ ]GaFSC(suc-c(RGDfK))<sub>3</sub> and [ $^{68}\text{Ga}$ ]GaNODAGA-c(RGDfK), and studied the effect of multivalency on targeting characteristics.

Cyclic RDGfK was prepared and modified at the  $\epsilon$ -amino function with 5-azidopentanoic acid to obtain c(RGDfK)N<sub>3</sub> containing an azide group for CuAAC. Terminal alkynyl moieties, which are compatible with the azide, were introduced to [Fe]FSC, [Fe]MAFC, and [Fe]DAFC.

The yields from conjugation of c(RGDfK)<sub>3</sub> with alkynyl[Fe]FSC or its derivatives *via* CuAAC were almost quantitative and subsequent demetalation were about 85% as confirmed by HPLC monitoring (see also Supporting Information Fig. S4). Finally, products FSC-based c(RGDfK)aza were successfully obtained in 30-37% overall yields after purification and could further be radiolabeled with <sup>68</sup>Ga in quantitative yields. Losses were mainly due to the demetalation and the final HPLC purification step, this could potentially be refined using alternative strategies. Removing iron before conjugation of the peptides, as used with other BFCs, Cu<sup>2+</sup> complexation by the click product could be a significant disadvantage. Using chelate cages such as sulfur and cyanide for copper removal may result in the cleavage of disulfide bonds in biomolecules and toxicity issues, respectively. Recently, Notni et al. established a method for removal of Cu<sup>2+</sup> from TRAP-conjugates after click reaction by using NOTA as a transchelator [30]. Using FSC and derivatives as iron-complex form, whereby the chelating moiety was fully occupied by Fe<sup>3+</sup>, Cu<sup>2+</sup> was unable to bind to the conjugation product. Additionally, we used an excess amount of chelating ligand THPTA, which tightly bound to Cu<sup>2+</sup>/Cu<sup>+</sup>, to protect Cu<sup>+</sup> from oxygen. This ensured removal of excess of Cu<sup>2+</sup> in one step together with removal of iron after the CuAAC click reaction by means of EDTA, thereby simplifying this approach.

The log*D* values (-2.96 to -3.80) revealed a high hydrophilicity of all compounds that was diminished with increasing number of c(RGDfK) moieties. Monomeric [<sup>68</sup>Ga]GaDAFC(c(RGDfK)aza) displayed a slightly higher hydrophilicity than standard [<sup>68</sup>Ga]GaNODAGA-c(RGDfK) (-3.80 vs -3.6) [7] whereas trimeric [<sup>68</sup>Ga]GaFSC(c(RGDfK)aza)<sub>3</sub> revealed lower hydrophilicity than the reference [<sup>68</sup>Ga]GaFSC(suc-c(RGDfK))<sub>3</sub> (-2.96 vs -3.6) [15]. These deviations can be explained by the hydrophilicity of the FSC scaffold and lipophilicity of the carbon chain and the 1*H*-1,2,3-triazole

linker, respectively. Protein binding that increased slightly with larger number of c(RGDfK) moieties was generally low with values between 3.3 to 8.9%. Stability tests in serum and PBS demonstrated the stability of all conjugates up to 2 h, thus, indicating their suitability for imaging over periods matching the half-life of gallium-68.

The determined  $IC_{50}$  values from displacement assays demonstrated the expected enhancement of the binding affinity to  $\alpha_v\beta_3$  integrin in the series mono-, di-, and trimeric c(RGDfK), which is in line with findings using a NOTA-based scaffold [26]. This was confirmed by internalization assays in  $\alpha_v\beta_3$ -positive M21 cells where the trimeric RGD derivatives showed higher cell uptake than di- and monomeric analogues, respectively (Fig. 2). Receptor-specificities of all conjugates were evidenced by low uptake values (0.2 to 0.7%) in M21 cells with blockade and M21-L ( $\alpha_v\beta_3$ -negative) cells. However, in U87MG cells lower values for the trimer were found with only 2.6% vs 2.9% for the dimer and 1.2% for the monomer. The overall lower values, despite using higher numbers of U87MG cells as compared to M21 cells, also confirms the reported lower receptor expression in this cell line [31].

*In vivo* behavior in SCID mice bearing  $\alpha_v\beta_3$ -positive U87MG glioblastoma xenograft provided expected enhancement of tumor accumulation of the trimer [ $^{68}\text{Ga}$ ]GaFSC(c(RGDfK)aza)<sub>3</sub> compared to monomeric [ $^{68}\text{Ga}$ ]GaDAFC(c(RGDfK)aza) and [ $^{68}\text{Ga}$ ]GaNODAGA-c(RGDfK), which was in line with our original findings with [ $^{68}\text{Ga}$ ]GaFSC(suc-c(RGDfK))<sub>3</sub>. Nonetheless, for dimeric [ $^{68}\text{Ga}$ ]GaMAFC(c(RGDfK)aza)<sub>2</sub> by far the highest uptake in U87MG tumors was found with  $8.19 \pm 0.41$  %ID/g. This trend was confirmed by microPET/CT imaging. It is in contrast to the higher affinity to  $\alpha_v\beta_3$ -Integrin and the more efficient binding affinity to M21 cells of the trimer. This observation could be explained by the lower density of  $\alpha_v\beta_3$ -integrins on U87MG cells and was partly confirmed by *in*

*vitro* binding results. It also should be noted that the increase in binding affinity between di- and trimeric FSC-RGD conjugates was less pronounced than between monomer and dimer. Likewise, Liu has proved that one of the most important factors for the increase of  $\alpha_v\beta_3$  affinity of multimeric cyclic RGD is bivalency [26,32]. Another reason for the better *in vivo* tumour targeting of dimeric [ $^{68}\text{Ga}$ ]GaMAFC(suc-c(RGDfK))<sub>2</sub> over trimeric [ $^{68}\text{Ga}$ ]GaFSC(c(RGDfK)aza)<sub>3</sub> could be related to differences in pharmacokinetics, i.e. better and more rapid diffusion into tissue due to lower steric hindrance of a smaller molecule, lower protein binding values, and lower lipophilicity, having a larger effect than the enhancement of  $\alpha_v\beta_3$  integrins binding affinity by additional RGD motifs.

In contrast, kidney uptake, blood and other major organ values increased as expected with increasing multimerization and were very comparable for the respective monomers and trimers. Exceptions were observed in spleen, which showed the highest accumulation for the dimer [ $^{68}\text{Ga}$ ]GaMAFC(c(RGDfK)aza)<sub>2</sub>, as well as liver, intestine, and stomach, which exhibited comparable uptakes for [ $^{68}\text{Ga}$ ]GaMAFC(c(RGDfK)aza)<sub>2</sub> and [ $^{68}\text{Ga}$ ]GaFSC(c(RGDfK)aza)<sub>3</sub>. These four organs are known to express  $\alpha_v\beta_3$  integrin [9], supporting the higher targeting efficiency of [ $^{68}\text{Ga}$ ]GaMAFC(c(RGDfK)aza)<sub>2</sub>. These improved targeting properties resulted in the highest tumor-to-tissue ratios among all investigated compounds.

Also some other studies showed that multivalency does not always improve the *in vivo* tumor uptake. Notni et al. [33] developed  $^{68}\text{Ga}$ -labeled prostate-specific membrane antigen (PSMA) inhibitor conjugates, using TRAP as a chelator and scaffold. Gallium-68 labeled mono-, di-, and trimeric lysine-urea-glutamic motifs (DBCO<sub>1</sub>, DBCO<sub>2</sub>, DBCO<sub>3</sub>) exhibited comparable tumor uptake in imaging studies, even slightly higher for the dimer. The reduced tumor accumulation of the trimer [ $^{68}\text{Ga}$ ]GaDBCO<sub>3</sub> was explained by the influence of molar total administrated amount

of biologically active compound. The authors concluded in their paper that molar activity had a more pronounced influence than structural and *in vitro* parameters. The applied molar activity in our study may therefore not have been optimal for all compounds.

Trimeric compounds showing lower tumor uptakes than dimeric counterpart were also observed in our previous work with the FSC scaffold [20,34]. Multimeric minigastrin analogues were prepared and tested *in vitro* and *in vivo*. At the studied time point, 1 h, dimeric conjugates exhibited higher tumor accumulations than the trimeric conjugates in biodistribution studies. At longer observation periods (2 h and 4 h) trimers revealed improved tumor uptake values. These results may support our data on [<sup>68</sup>Ga]GaFSC(c(RGDfK)aza)<sub>3</sub> at 90 min p.i., possibly not long enough for optimal target accumulation.

In a recent comparison of 4 different di- and trimeric RGD-conjugates including [<sup>68</sup>Ga]GaFSC(suc-c(RGDfK))<sub>3</sub>, the highest tumor targeting was found for trimeric compounds, however a dimeric [<sup>68</sup>Ga]GaDOTA-E-[c(RGDfK)]<sub>2</sub> revealed similar tumor-to-tissue ratios as compared to its trimeric counterparts and the difference was more pronounced in a tumor model with higher expression of  $\alpha_v\beta_3$  integrins [11]. The potential effect of simultaneous binding of more than one RGD unit to  $\alpha_v\beta_3$  integrins by multimeric RGD tracers seemed to be unlikely due to limited spacer length between the RGD units [26].

## 5. Conclusion

Mono- and multimeric RGD bioconjugates based on the FSC scaffold were directly accessible applying click chemistry. The dimeric [<sup>68</sup>Ga]GaMAFC(c(RGDfK)aza)<sub>2</sub> was found to be superior to the trimeric [<sup>68</sup>Ga]GaFSC(c(RGDfK)aza)<sub>3</sub> due to its higher tumor uptake and tumor-to-tissue

ratios *in vivo* together with highest visualization intensity in PET/CT imaging. Although trimeric [<sup>68</sup>Ga]GaFSC(c(RGDfK)aza)<sub>3</sub> demonstrated the highest α<sub>v</sub>β<sub>3</sub>-integrin affinity *in vitro*, its *in vivo* tumor-to-tissue ratios were even poorer than the monomeric [<sup>68</sup>Ga]GaDAFC(c(RGDfK)aza). Multivalency improved binding affinity from mono- to di- and mono- to tri-, but not from di- to trimeric counterparts. Bivalency was dominant over the multivalency in this study. However, different trends may be observed in other cases depending on the molecular structure, type of BFC, and cyclic RGD arrangement. [<sup>68</sup>Ga]GaMAFC(c(RGDfK)aza)<sub>2</sub> shows promising characteristics for angiogenesis imaging, and it could be further applied to dual-targeting by introducing an additional targeting moiety to the FSC scaffold.

#### **Conflict of interest**

The authors declare that they have no conflict of interest.

#### **Acknowledgements**

The authors gratefully acknowledge the financial support of the Royal Thai Government Scholarships (PhD scholarship to P. Kaeopookum), the Austrian Science Foundation (FWF; grant P 25899-B23 to C. Decristoforo and Euregio SupErA IPN95-B30 to H. Haas), Ministry of Education, Youth and Sports of the Czech Republic (LO1304; to M. Petrik) and European Regional Development Fund - Project ENOCH (No. CZ.02.1.01/0.0/0.0/16\_019/0000868; to M. Petrik). We would like to thank Heinz Zoller and Nadja Baumgartner, Department of Internal Medicine II, Medical University Innsbruck, for making MALDI-TOF analysis available and Leo Gruber, Department of Radiology, Medical University Innsbruck for support in statistical evaluation.

**Appendix A. Supplementary data**

Fig. S1 showing the internalization studies in U87MG cell line at 90 min incubation

Fig. S2 comparing relative tracer uptake in U87MG tumor of all RGD peptides at 90 min p.i.

Fig. S3 showing the tumor-to-tissue ratios of [<sup>68</sup>Ga]Ga-c(RGDfK)aza in SCID mice bearing U87MG tumor at 30 min p.i.

Fig. S4 showing HPLC monitoring of click reaction and iron removal of [Fe]DAFC(c(RGDfK)aza)

**References**

- [1] Folkman J. Role of angiogenesis in tumor growth and metastasis. *Semin Oncol* 2002;29: 15–8.
- [2] Brooks PC, Strömblad S, Klemke R, Visscher D, Sarkar FH, Cheresh DA. Antiintegrin alpha v beta 3 blocks human breast cancer growth and angiogenesis in human skin. *J Clin Invest* 1995;96:1815–22.
- [3] Brooks PC, Clark RA, Cheresh DA. Requirement of vascular integrin alpha v beta 3 for angiogenesis. *Science* 1994;264:569–71.
- [4] Kumar CC. Integrin alpha v beta 3 as a therapeutic target for blocking tumor-induced angiogenesis. *Curr Drug Targets* 2003;4:123–31.
- [5] Haubner R, Beer AJ, Wang H, Chen X. Positron emission tomography tracers for imaging angiogenesis. *Eur J Nucl Med Mol Imaging* 2010;37:S86–103.

- [6] Jeong JM, Hong MK, Chang YS, Lee YS, Kim YJ, Cheon GJ, et al. Preparation of a promising angiogenesis PET imaging agent:  $^{68}\text{Ga}$ -labeled c(RGDyK)-isothiocyanatobenzyl-1,4,7-triazacyclononane-1,4,7-triacetic acid and feasibility studies in mice. *J Nucl Med* 2008;49:830–6.
- [7] Knetsch PA, Petrik M, Griessinger CM, Rangger C, Fani M, Kesenheimer C, et al. [ $^{68}\text{Ga}$ ]NODAGA-RGD for imaging  $\alpha_v\beta_3$  integrin expression. *Eur J Nucl Med Mol Imaging* 2011;38:1303–12.
- [8] Dumont RA, Deininger F, Haubner R, Maecke HR, Weber WA, Fani M. Novel  $^{64}\text{Cu}$ - and  $^{68}\text{Ga}$ -labeled RGD conjugates show improved PET imaging of  $\alpha_v\beta_3$  integrin expression and facile radiosynthesis. *J Nucl Med* 2011;52:1276–84.
- [9] Notni J, Pohle K, Wester HJ. Be spoilt for choice with radiolabelled RGD peptides: preclinical evaluation of  $^{68}\text{Ga}$ -TRAP(RGD) $_3$ . *Nucl Med Biol* 2013;40:33–41.
- [10] Knetsch PA, Zhai C, Rangger C, Blatzer M, Haas H, Kaeopookum P, et al. [ $^{68}\text{Ga}$ ]FSC-(RGD) $_3$ , a trimeric RGD peptide for imaging  $\alpha_v\beta_3$  integrin expression based on a novel siderophore derived chelating scaffold—synthesis and evaluation. *Nucl Med Biol* 2015;42:115–22.
- [11] Lobeek D, Franssen GM, Ma MT, Wester HJ, Decrisoforo C, Oyen WJG, et al. In vivo characterization of 4  $^{68}\text{Ga}$ -labeled multimeric RGD peptides to image  $\alpha_v\beta_3$  integrin expression in 2 human tumor xenograft mouse models. *J Nucl Med* 2018;59: 1296–301.
- [12] Wängler C, Maschauer S, Prante O, Schäfer M, Schirmacher R, Bartenstein P, et al. Multimerization of cRGD peptides by click chemistry: synthetic strategies, chemical limitations, and influence on biological properties. *ChemBioChem* 2010;11:2168–81.

- [13] Dijkgraaf I, Yim CB, Franssen GM, Schuit RC, Luurtsema G, Lui S, et al. PET imaging of  $\alpha_v\beta_3$  integrin expression in tumours with  $^{68}\text{Ga}$ -labelled mono-, di- and tetrameric RGD peptides. *Eur J Nucl Med Mol Imaging* 2011;38:128–37.
- [14] Li ZB, Chen K, Chen X.  $^{68}\text{Ga}$ -labeled multimeric RGD peptides for microPET imaging of integrin  $\alpha_v\beta_3$  expression. *Eur J Nucl Med Mol Imaging* 2008;35:1100–8.
- [15] Zhai C, Franssen GM, Petrik M, Laverman P, Summer D, Rangger C, et al. Comparison of Ga-68-labeled fusarinine C-based multivalent RGD conjugates and [ $^{68}\text{Ga}$ ]NODAGA-RGD—in vivo imaging studies in human xenograft tumors. *Mol Imaging Biol* 2016;18:758–67.
- [16] Summer D, Grossrubatscher L, Petrik M, Michalcikova T, Novy Z, Rangger C, et al. Developing targeted hybrid imaging probes by chelator scaffolding. *Bioconjugate Chem* 2017;28:1722–33.
- [17] Zhai C, Summer D, Rangger C, Haas H, Haubner R, Decristoforo C. Fusarinine C, a novel siderophore-based bifunctional chelator for radiolabeling with Gallium-68. *J Labelled Comp Radiopharm* 2015;58:209–14.
- [18] Petrik M, Zhai C, Novy Z, Urbanek L, Haas H, Decristoforo C. In vitro and in vivo comparison of selected Ga-68 and Zr-89 labelled siderophores. *Mol Imaging Biol* 2016;18:344–52.
- [19] Kaeopookum P, Summer D, Pfister J, Orasch T, Lechner BE, Petrik M, et al. Modifying the siderophore triacetylfusarinine C for molecular imaging of fungal infection. *Mol Imaging Biol* 2019. doi: 10.1007/s11307-019-01325-6
- [20] Summer D, Kroess A, Woerndle R, Rangger C, Klingler M, Haas H, et al. Multimerization results in formation of rebindable metabolites: a proof of concept study with FSC-based

- minigastrin imaging probes targeting CCK2R expression. PLoS ONE 2018;13:e0201224.  
<https://doi.org/10.1371/journal.pone.0201224>
- [21] Schrettl M, Bignell E, Kragl C, Sabiha Y, Loss O, Eisendle M, et al. Distinct roles for intra- and extracellular siderophores during *Aspergillus fumigatus* infection. PLoS Pathog 2007;3:1195–207.
- [22] Haubner R, Wester HJ, Reuning U, Senekowitsch-Schmidtke R, Diefenbach B, Kessler H, et al. Radiolabeled  $\alpha_v\beta_3$  integrin antagonists: a new class of tracers for tumor targeting. J Nucl Med 1999;40:1061–71.
- [23] Haubner R, Wester HJ, Burkhart F, Senekowitsch-Schmidtke R, Weber W, Goodman SL, et al. Glycosylated RGD-containing peptides: tracer for tumor targeting and angiogenesis imaging with improved biokinetics. J Nucl Med 2001;42: 326–36.
- [24] Decristoforo C, Gonzalez IH, Carlsen J, Rupprich M, Huisman M, Virgolini I, et al.  $^{68}\text{Ga}$ - and  $^{111}\text{In}$ -labelled DOTA-RGD peptides for imaging of  $\alpha_v\beta_3$  integrin expression. Eur J Nucl Med Mol Imaging 2008;35:1507–15.
- [25] Liu S. Radiolabeled multimeric cyclic RGD peptides as integrin  $\alpha_v\beta_3$  targeted radiotracers for tumor imaging. Mol Pharm 2006;3:472–87.
- [26] Liu S. Radiolabeled cyclic RGD peptide bioconjugates as radiotracers targeting multiple integrins. Bioconjugate Chem 2015;26:1413–38.
- [27] Notni J, Simecek J, Hermann P, Wester HJ. TRAP, a powerful and versatile framework for gallium-68 radiopharmaceuticals. Chem Eur J 2011;17:14718–22.
- [28] Kriemen E, Ruf E, Behrens U, Maison W. Synthesis of 1,4,7,10-Tetra-azacyclododecan-1,4,7,10-tetra-azidoethylacetic acid (DOTAZA) and related “clickable” DOTA derivatives. Chem Asian J 2014;9:2197–202.

- [29] Makarem A, Klika KD, Litau G, Remde Y, Kopka K. HBED-NN: a bifunctional chelator for constructing radiopharmaceuticals. *J Org Chem* 2019;84:7501–8.
- [30] Baranyai Z, Reich D, Vagner A, Weineisen M, Toth I, Wester HJ, Notni J. A shortcut to high-affinity Ga-68 and Cu-64 radiopharmaceuticals: one-pot click chemistry trimerisation on the TRAP platform. *Dalton Trans* 2015;44:11137–46.
- [31] Goodman SL, Grote HJ, Wilm C. Matched rabbit monoclonal antibodies against  $\alpha$ v-series integrins reveal a novel  $\alpha$ v $\beta$ <sub>3</sub>-LIBS epitope, and permit routine staining of archival paraffin samples of human tumors. *Biol Open* 2012;1:329–40.
- [32] Chakraborty S, Liu S, Kim YS, Shi J, Zhou Y, Wang F. Evaluation of <sup>111</sup>In-labeled cyclic RGD peptides: tetrameric not tetravalent. *Bioconjugate Chem* 2010;21:969–78.
- [33] Wurzer A, Pollman J, Schmidt A, Reich D, Wester HJ, Notni J. Molar activity of Ga-68 labeled PSMA inhibitor conjugates determines PET imaging results. *Mol Pharm* 2018;15:4296–302.
- [34] Summer D, Rangger C, Klingler M, Laverman P, Franssen GB, Lechner BE, et al. Exploiting the concept of multivalency with <sup>68</sup>Ga- and <sup>89</sup>Zr-labelled fusarinine C-minigastrin bioconjugates for targeting CCK2R expression. *Contrast Media Mol Imaging* 2018; <https://doi.org/10.1155/2018/3171794>

**Table 1**

Distribution coefficient ( $\log D$ ), protein binding, and stability in PBS (pH 7.4) and human serum of mono-, di-, and trimeric [<sup>68</sup>Ga]Ga-c(RGDfK)aza.

[ <sup>68</sup> Ga]Ga-c(RGDfK)aza	$\log D$ ( $n = 6$ )	Incubation time ( $n = 3$ )	Protein binding (%) ( $n = 3$ )	Stability (% RCP)	
				PBS ( $n = 3$ )	serum ( $n = 3$ )
[ <sup>68</sup> Ga]GaDAFC(c(RGDfK)aza)	-3.80 ± 0.06	30	4.6 ± 0.7	99.9 ± 0.0	99.6 ± 0.2
		60	3.4 ± 0.0	99.8 ± 0.1	99.7 ± 0.1

		120	$3.3 \pm 0.8$	$99.6 \pm 0.3$	$99.3 \pm 0.6$
$[^{68}\text{Ga}]\text{GaMAFC}(\text{c}(\text{RGDfK})\text{aza})_2$	$-3.54 \pm 0.11$	30	$5.8 \pm 0.7$	$99.7 \pm 0.1$	$99.8 \pm 0.2$
		60	$6.2 \pm 0.7$	$99.9 \pm 0.0$	$99.8 \pm 0.2$
		120	$7.2 \pm 0.9$	$99.8 \pm 0.1$	$99.5 \pm 0.3$
$[^{68}\text{Ga}]\text{GaFSC}(\text{c}(\text{RGDfK})\text{aza})_3$	$-2.96 \pm 0.21$	30	$8.3 \pm 0.6$	$99.7 \pm 0.3$	$99.8 \pm 0.2$
		60	$8.7 \pm 0.8$	$99.4 \pm 0.4$	$99.7 \pm 0.2$
		120	$8.9 \pm 1.1$	$99.5 \pm 0.6$	$99.3 \pm 0.7$

---

Journal Pre-proof



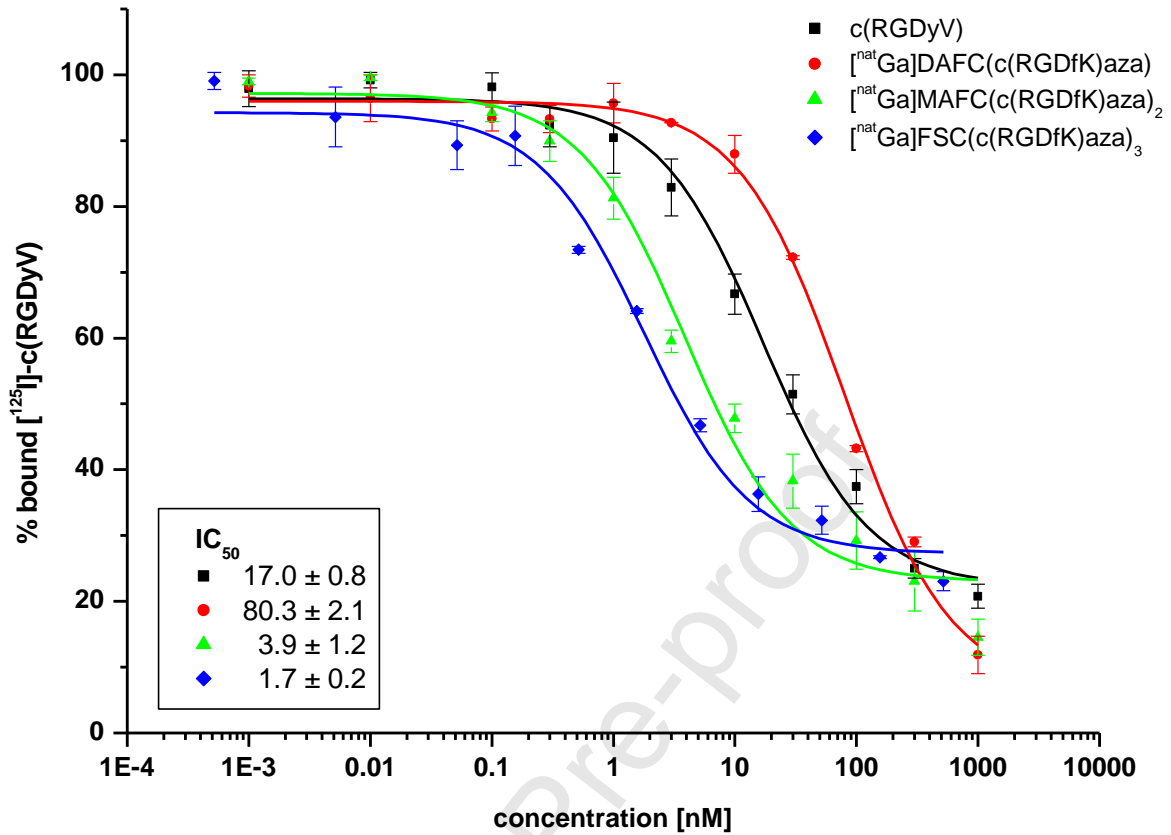


**Fig. 1.** Competition assay of mono-, di-, and trimeric  $[^{\text{nat}}\text{Ga}]\text{-c(RGDfK)aza}$  versus  $[^{125}\text{I}]\text{c(RGDyV)}$  radioligand on human melanoma M21 ( $\alpha_v\beta_3$ -positive) cells (mean  $\pm$  SD,  $n = 3$ ) including  $\text{IC}_{50}$  values (binding affinity).

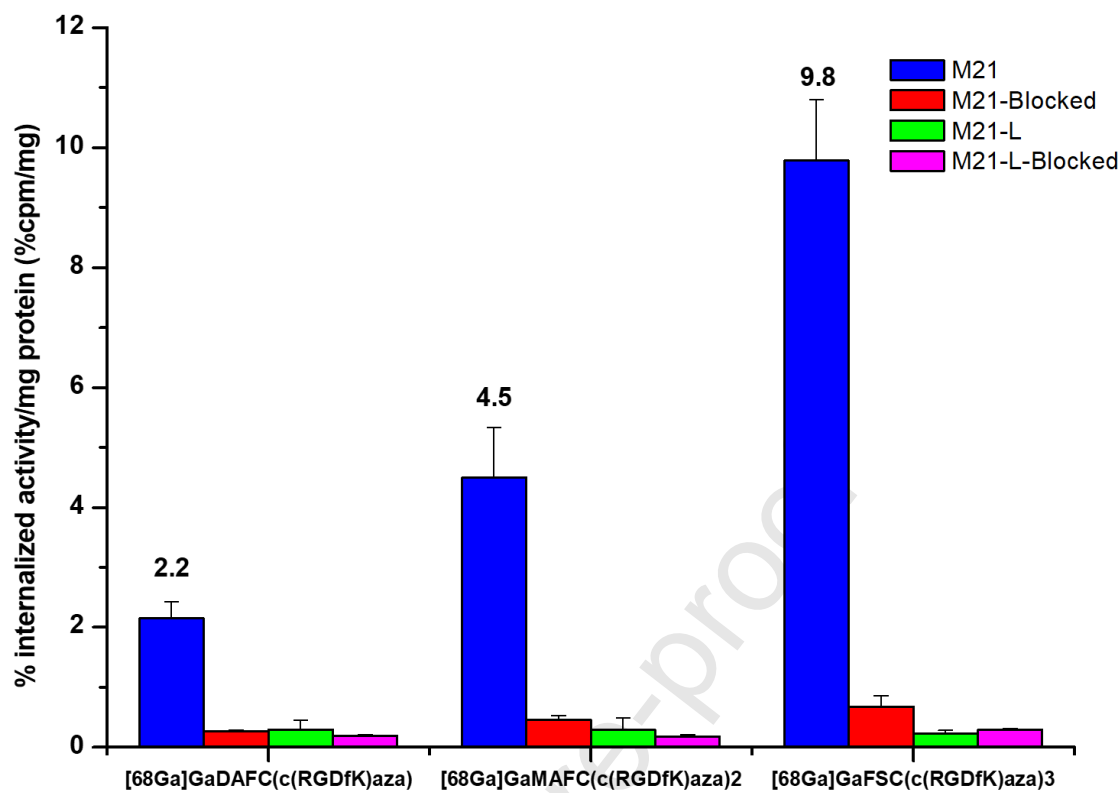


**Fig. 2.** *In vitro* uptake of  $^{68}\text{Ga}$ -labeled c(RGDfK)aza in human melanoma M21 ( $\alpha_v\beta_3$ -positive) and M21-L ( $\alpha_v\beta_3$ -negative) cells with or without blocking solution (10  $\mu\text{M}$  c(RGDyV)) at 37  $^{\circ}\text{C}$  for 90 min ( $n = 3$ ).

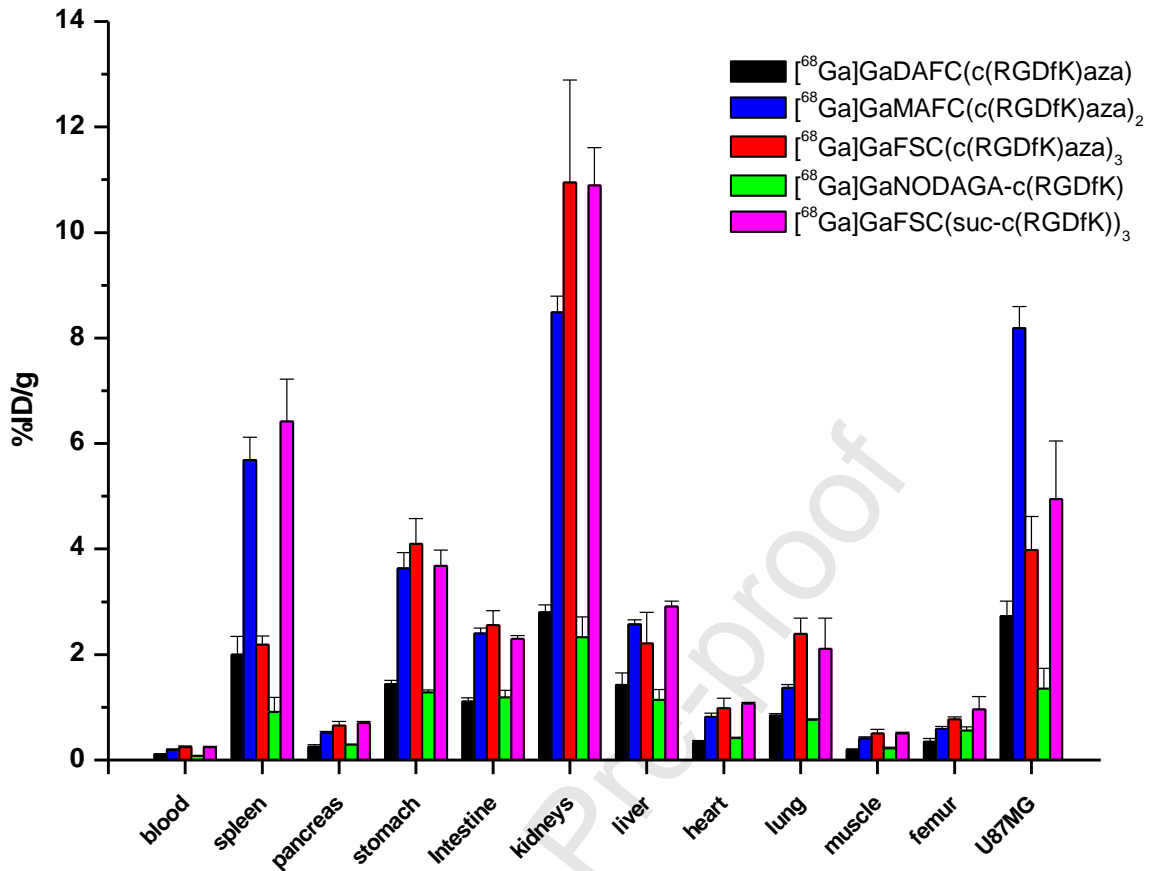
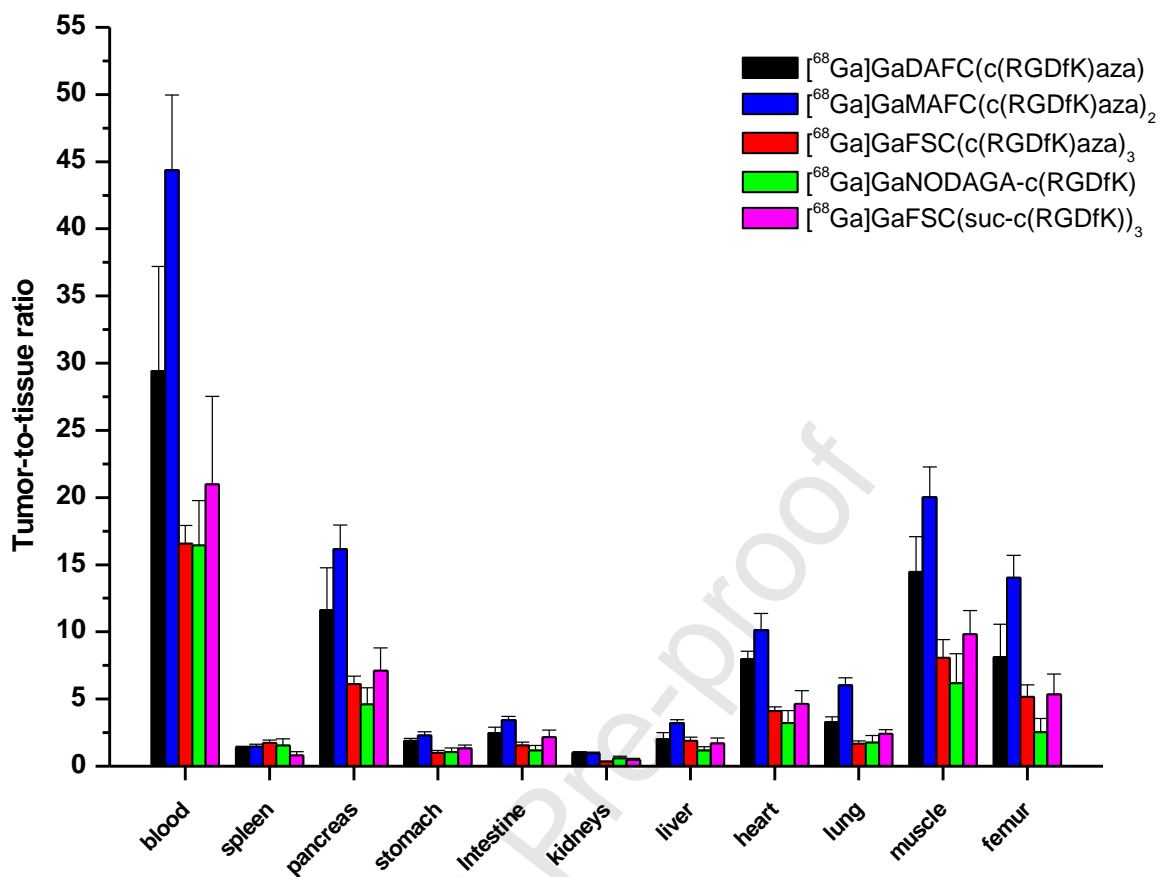
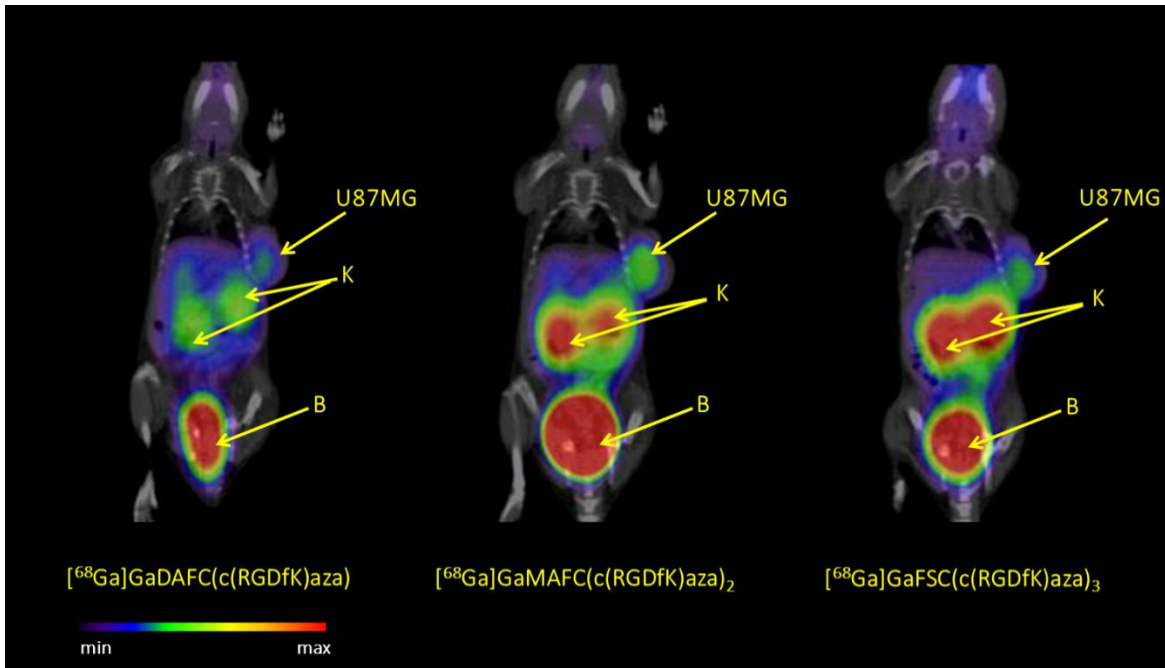


Fig.

3. Biodistribution in SCID mice bearing U87MG tumor ( $\alpha_v\beta_3$ -positive) of mono-, di-, and trimeric [<sup>68</sup>Ga]Ga-c(RGDfK)aza compared with monomeric [<sup>68</sup>Ga]GaNODAGA-c(RGDfK) and trimeric [<sup>68</sup>Ga]GaFSC(suc-c(RGDfK))<sub>3</sub> at 90 min p.i. ( $n = 3$ ). Tissue uptake values are presented as the percentage of injected dose per gram of tissue (%ID/g).



**Fig. 4.** Comparison of tumor-to-tissue ratios of mono-, di-, and trimeric [ $^{68}\text{Ga}$ ]Ga-c(RGDfK)aza in SCID mice bearing U87MG tumor ( $\alpha_v\beta_3$ -positive) at 90 min p.i. ( $n = 3$ ).



**Fig. 5.** Static microPET/CT images in SCID mice bearing U87MG tumor ( $\alpha_v\beta_3$ -positive) of mono-, di-, and trimeric  $[^{68}\text{Ga}]\text{Ga-c}(\text{RGDfK})\text{aza}$  at 90 min p.i. under 2% isoflurane anaesthesia: fused PET/CT coronal slices (prone position) (approx. 5–8 MBq injected dose; *B*-bladder, *K*-kidney).